The Enge Split-Pole Spectrograph at the University of Notre Dame

Scott Carmichael[1*], *Patrick* O'Malley[1**], *Daniel* Bardayan[1], *Thomas* Bailey[1], *Chevelle* Boomershine[1], *Maxime* Brodeur[1], *Sydney* Coil[1], *Cade* Dembski[1], *Tom* Gore[1], *Chloe* Jones[1], *Jes* Koros[1], *Kevin* Lee[1], *Pedro Luiz* Domingues Magro[1,2], *John* McDonaugh[1], *Griffin* Mulcahy[1], *William* Porter[1], *Fabio* Rivero[1], *Daniel* Robertson[1], *Javier* Rufino[1], *Adam* Sanchez[1], *Edward* Stech[1], *William* von Seeger[1], and *Regan* Zite[1,]

[1]Department of Physics and Astronomy, University of Notre Dame, Notre Dame, Indiana 46556, USA
[2]Instituto de Física, Universidade de São Paulo, Rua do Matão 1371, São Paulo, SP 05508-090, Brazil

Abstract. Nuclear reactions play a crucial role in determining the nucleosynthesis that occurs in astrophysical events. The rates of many reactions that significantly impact certain nucleosynthesis processes can not be currently measured via direct means. These reactions must be constrained in another manner, such as determining the level energies and other structure properties of the compound nuclei. In order to measure level energies of nuclei relevant to nuclear astrophysics, the Enge split-pole spectrograph has been installed and commissioned at the University of Notre Dame's Nuclear Science Laboratory. The first scientific measurement has also been performed. Structure properties of ^{58}Cu were measured via the reaction ^{58}Ni(^{3}He,t)^{58}Cu to provide the first experimental constraint of the ^{57}Ni(p,γ)^{58}Cu reaction rate, which impacts the production of of ^{44}Ti, ^{57}Fe, and ^{59}Ni in core-collapse supernovae. Preliminary analysis of this measurement confirms the level energies of states in ^{58}Cu that could lead to significant resonances in the ^{57}Ni(p,γ)^{58}Cu reaction rate, while suggesting the presence of additional states that have not been previously observed but could also lead to significant resonances.

1 Introduction

A primary goal of nuclear astrophysics is to understand the nucleosynthesis processes that created the elements and the environments in which these processes occur. For many environments, there are certain reaction rates that have a more significant impact than others on the resulting nucleosynthesis. To identify which nuclei are synthesized in a certain environment, it is then necessary to determine these significant reaction rates.

Many important nucleosynthesis processes occur in explosive, high-temperature environments such as novae, x-ray bursts, and supernovae. The higher the temperature, the higher the average interaction energy between nuclei. As the interaction energy increases, it becomes more likely that resonance reactions will occur, which proceed through excited states in the compound nucleus. For many nuclear reactions, it is not currently feasible to experimentally measure the rate directly. However, the strength of these resonances, and thus the overall nuclear reaction rate, will be determined by the structure of the compound nucleus. It is therefore possible to indirectly constrain the nuclear reaction rate by measuring structure properties of the nucleus of interest.

Different methods exist to indirectly constrain the reaction rate. The method best suited to constrain a particular reaction rate will partially be determined by the density of nuclear states within the region of excitation energy where resonances will most significantly contribute. If the level density is low (<10 levels/MeV) and the resonance width is sufficiently narrow, then the reaction rate can be experimentally constrained via the narrow resonance formalism. In this formalism it is assumed that the resonance is narrow enough to where the interaction energy will not vary over the width of the resonance. With this approximation, the reaction rate per particle pair (in cm^3 mole^{-1} s^{-1}) takes the form [1]:

$$N_A\langle\sigma\nu\rangle = 1.54\times10^{11}(\mu T_9)^{-3/2}\sum_i(\omega\gamma)_i e^{-11.605E_i/T_9} \quad (1)$$

where the sum is over all narrow resonances, μ is reduced mass in amu, T_9 is temperature in GK, $(\omega\gamma)_i$ and E_i are strength and energy of resonance i in units of MeV, respectively. The resonance strength is defined as

$$\omega\gamma = \frac{2J_r+1}{(2J_1+1)(2J_2+1)}\frac{\Gamma_a\Gamma_b}{\Gamma_r}$$

where J_r, J_1, J_2 are the spins of the compound nucleus and reaction products. $\Gamma_r, \Gamma_a, \Gamma_b$ are the total width of the resonance, and the decay widths of entrance and exit channel, respectively.

In this formalism, the reaction rate is exponentially dependent on resonance energy, meaning it is exponentially dependent on the level energies of the compound nucleus. To effectively constrain the reaction rate, it is then crucial to precisely determine the level energies of the compound nucleus. Further structure information, such as the spin

*e-mail: scarmic1@nd.edu
**e-mail: pomalle4@nd.edu

and decay widths of states in the compound nucleus are also important.

A specific example in which this type of constraint would be necessary is the ^{57}Ni(p,γ)^{58}Cu reaction rate. This rate is significant because it has been shown to impact the production of ^{44}Ti, ^{57}Fe, and ^{59}Ni in core-collapse supernovae (CCSNe) [2–4].

The yield of ^{44}Ti in CCSNe can be inferred from the observation of gamma-rays in the CCSNe remnant, making it an important probe into the dynamics of these events. Magkotsios *et. al.* performed a nucleosynthesis sensitivity study using nuclear network calculations and demonstrated that increasing or decreasing the reaction rate of ^{57}Ni(p,γ)^{58}Cu by a factor of 100 impacts the ^{44}Ti production by a factor of 10 or more at some point in the evolution of the network [2].

In a more recent sensitivity study, Hermansen *et. al.* also found that varying the rate of ^{57}Ni(p,γ)^{58}Cu impacts the production of ^{44}Ti, but to a lesser extent than Magkotsios *et. al*. Varying the rate by a factor of 100 fell just under the threshold of what they considered significant, which was a change in the final abundance of ^{44}Ti by a factor of 1.1 or greater (essentially a 10% change) [3]. However, this study also noted that decreasing the ^{57}Ni(p,γ)^{58}Cu reaction rate by a factor of 100 decreased the production of ^{59}Ni by a factor of 1.27. This is significant because determining the amount of ^{59}Ni produced in CCSNe is needed to test models of cosmic ray acceleration.

It should be noted that another recent sensitivity study by Subedi *et. al.* did not notice an impact on ^{44}Ti production when varying the ^{57}Ni(p,γ)^{58}Cu reaction rate [5]. However, this is likely due to the fact that the authors assumed the reaction rate was well constrained by the theoretical calculations, and only varied the reaction rate by a factor of 10. As will be seen, this assumption is questionable for this scenario.

Finally, in a sensitivity study on the impact of nuclear reaction rates on νp-process nucleosynthesis, Nishimura *et. al.* found that the ^{57}Ni(p,γ)^{58}Cu reaction significantly impacts ^{57}Fe production. While the astrophysical site of the νp-process is still unknown, candidate cites include CCSNe. This study varied reaction rates for 23 parameterized thermodynamic trajectories that covered a wide range of possible νp-process conditions. In 13 of these 23 trajectories, the ^{57}Ni(p,γ)^{58}Cu reaction rate was shown to impact ^{57}Fe production [4]. By number of trajectories impacted, this tied for the third most significant reaction identified in the study.

Understanding how the isotopes ^{44}Ti, ^{57}Fe, and ^{59}Ni are produced is important in determining the nucleosynthesis processes that occur in CCSNe. However, despite this importance, no experimental rates exist for the ^{57}Ni(p,γ)^{58}Cu reaction. Current theoretical rates for the reaction are based off of Hauser-Feshbach statistical model calculations, but the validity of these calculations is questionable. Low spin states in the compound nucleus, ^{58}Cu, between 3 and 6 MeV are expected to contribute to resonances in the reaction. Table 1 lists the current known levels in ^{58}Cu between 3 and 6 MeV [6]. As can be seen, the level density of low spin states in this region falls below 10 levels/MeV, which is generally taken to be the threshold of Hauser-Feshbach model validity. Additional study into the structure of ^{58}Cu in the 3 to 6 MeV excitation range is thus necessary to determine the validity of the theoretical calculations.

To provide the capabilities to measure structure properties of ^{58}Cu, and other nuclei significant to nuclear astrophysics, an Enge split-pole spectrograph was installed at the University of Notre Dame's Nuclear Science Laboratory [7]. The Enge split-pole spectrograph is an ideal tool to perform this study, as it will provide precise measurements of the ^{58}Cu level energies to be used in constraining the rate via the narrow resonance formalism if the level density does fall below 10 levels/MeV.

Table 1: Energy and spin-parity of known states in ^{58}Cu between 3 and 6 MeV [6].

E (keV)	J^π	E (keV)	J^π
3230 *10*		4065.6 *6*	(7+)
3280.2 *8*	(0+:4+)	4210 *20*	
3310 *20*		4441.4 *6*	(8+)
3421.0 *5*	(7+)	4720 *10*	(1)+
3460.1 *1*	(1)+	5065 *20*	(1)+
3512.6 *7*		5160 *20*	
3570 *20*		5190.6 *23*	(7+)
3677.9 *8*	(1)+	5348.0 *8*	(9+)
3717 *10*	(1)+	5451 *20*	(1)+
3820 *20*		5574.9 *8*	(9+)
3890 *20*		5645 *20*	(1)+
4010			

2 Enge Split-Pole Spectrograph

The Enge split-pole spectrograph that was installed at the Nuclear Science Laboratory is based on the design of H. A. Enge [8]. The spectrograph is a Scanditronix model ESP 90. Charged particles that are ejected from a nuclear reaction and enter the spectrograph will be separated and focused onto the focal plane based on their magnetic rigidity. The split-pole design creates a magnetic field that provides second-order transverse focusing and vertical focusing. In practice, this ensures that particles entering the spectrograph with the same magnetic rigidity but diverging angles will still be focused at the same point on the focal plane. This increases the angular acceptance of the device (8-12 msr) while still providing good resolving power ($p/\Delta p > 5000$) [7, 8]. A diagram of the device is shown in Figure 1.

By measuring the position of particles on the focal plane, the energy of the ejectile can be determined. From the ejectile energy and reaction kinematics, the level energies of the residual nucleus can be measured to high precision. While the resolution (and thus the precision) of the excitation spectrum will depend on the ejectile energy and

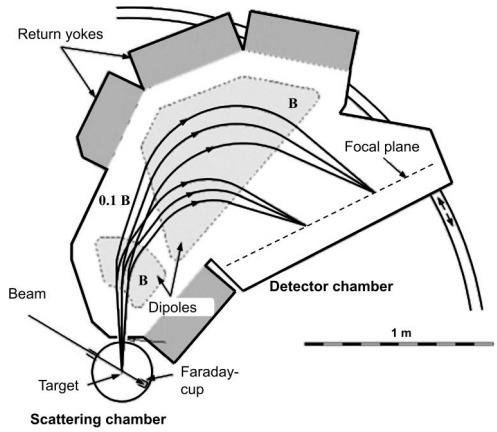

Figure 1: Diagram of the split-pole spectrograph as viewed from above. Particle rays demonstrate the effects of second order focusing. Adapted from [8].

the reaction in question, measurements of level energies to a precision of ~ 2-5 keV are expected.

In addition to measurements of level energies, the spectrograph is also capable of constraining other structure properties. The spectrograph can be rotated between 0° and 60° to measure angular distributions, which can be used to constrain the spin of states in the residual nucleus. Detectors can also be placed in the target chamber to detect charged particle decays of the residual nuclei in coincidence with the ejectiles. This allows for the measurement of particle branching ratios and the determination of particle widths of states in the residual nuclei. All of these capabilities make the Enge split-pole spectrograph an ideal tool for probing the structure of nuclei in order to constrain reaction rates relevant to nuclear astrophysics.

3 Detectors

3.1 Focal Plane Detectors

To effectively utilize the resolving power of the Enge split-pole spectrograph, a detector is required at the focal plane that is capable of a position resolution on the order of mm. To this end, a position sensitive ionization chamber was designed and constructed. This focal plane detector (FPD) was based on the design of the detector that was used with the Enge split-pole spectrograph originally located at Yale University's Wright Nuclear Structure Laboratory, though it is now at Florida State University's John D. Fox Accelerator Laboratory [9, 10]. While the detector was designed to measure light particles (such as H and He), in principle it could also be used to measure heavier particles.

The FPD consists of an entrance window, exit window, cathode, and two position-sensitive anode sections (one at the entrance and one at the exit). A diagram of the detector and its major components is shown in Figure 2. The position-sensitive sections each consist of three anode wires and a printed circuit board (PCB) assembly. The assembly consists of a PCB board that runs parallel to the plane created by the anode wires. On this PCB are a row of 220 conducting pads, each with a width of 2.286 mm and separated by 0.254 mm.

When a particle passes under the anode wires, it liberates electrons that are collected at the anode wires, and a charge is induced on the pick-up pads. Each one of these pick-pads is attached to a delay tap that delays the signal by 5 ns. Each delay tap is connected in series to form a delay line. The induced charge on the pick-up pads splits and travels to both ends of the delay line. By taking the timing difference between the signals on either end of the delay line, the position of the particle can be determined. A partial diagram of the anode wires and pick-up pads is shown in Figure 3.

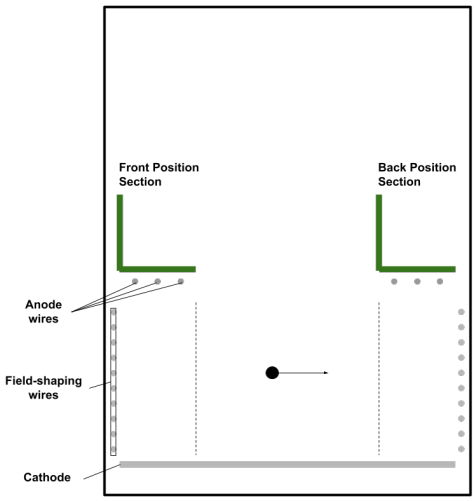

Figure 2: Diagram of the focal plane detector as viewed from the side.

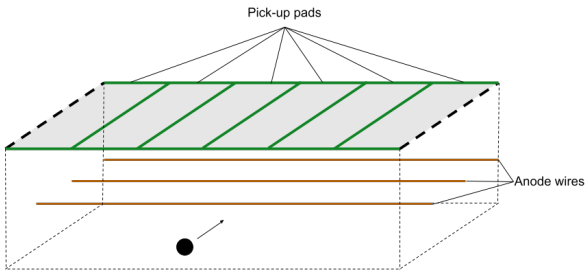

Figure 3: Section of anode wires and pick-up pads. Example of particle with direction of travel is shown.

Additionally, a plastic scintillator is placed behind the FPD to measure the residual energy of ejectiles after passing through the FPD. This residual energy measurement aids in particle identification, which is necessary to select the reaction channel of interest.

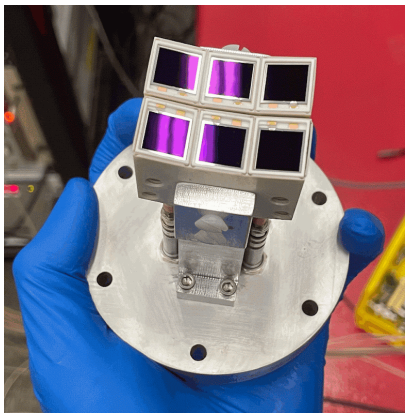

Figure 4: Flange-mounted array of silicon diode detectors used to detect charged particle decays from the residual nuclei.

3.2 Diode Detectors

An array of silicon diode detectors has been designed and constructed to be mounted on the target chamber flanges. Each flange-mounted array consists of 2 rows of 3 individual diode detectors with an angular spacing of 10°. The flanges are positioned on the beam-right side of the target chamber in 30° increments, allowing for the diode detectors to cover angles from 20° to 160° in 10° increments. These diode arrays will detect charged particle decays from the residual nucleus in coincidence with the ejectiles detected in the FPD. This will allow for charged particle branching ratios to be measured and charged particle widths of the resonance to be determined. A picture of a single diode array is shown in Figure 4.

4 Experimental Details

As of early 2024, the Enge Split-Pole Spectrograph at the University of Notre Dame is fully operational and the first scientific measurement has been performed. In order to probe the structure of ^{58}Cu in the 3-6 MeV excitation region, the ^{58}Ni(^{3}He,t)^{58}Cu reaction was measured.

A ^{3}He beam of 21 MeV was impinged on a (~200 μg/cm^{2} ^{58}Ni target with a thin ^{12}C backing, and the charge exchange reaction was used to populate states in ^{58}Cu. The tritons ejected in the reaction were separated using the spectrograph. From the position of the tritons on the focal plane, their energies could be determined and the level energies of states in ^{58}Cu could be measured. Data were collected at 6 different entrance angles of the spectrograph ranging from 14° to 35° in the laboratory frame. The analysis procedure and preliminary results are described in the following section.

5 Results

5.1 Elastic Scattering Data

To determine characteristics of both the spectrograph and the FPD, the ^{3}He elastic scattering peak was measured at an angle of ~14.5° and four different magnetic field settings. Because the bending radius of a particle is proportional to the magnetic field strength, these measurements were able to provide a calibration between the position on the focal plane and particle bending radius. The bending radius of the particle can then ultimately be used to determine its energy.

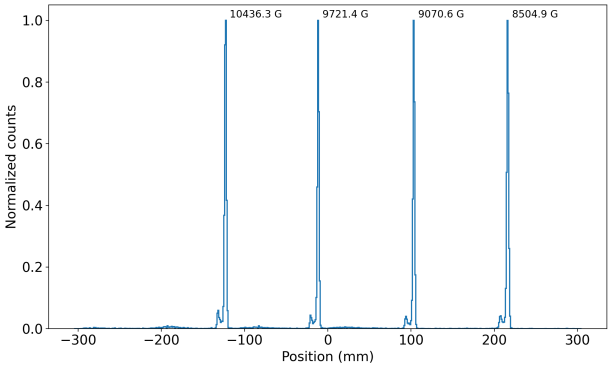

Figure 5: ^{3}He elastic scattering peaks labeled by the magnetic field strengths at which they were taken. The width of the peaks is approximately constant over the range of the detector, suggesting the detector was parallel with the focal plane. The peak heights are normalized to 1 for plotting purposes.

A plot of the position of the peaks at the four different magnetic field strengths is shown in Figure 5. The peaks have been normalized to a height of 1 for plotting purposes. At each magnetic field setting, a doublet was observed. This corresponded to ^{3}He scattering on ^{58}Ni (large peak) and ^{12}C (small peak). The width of the peak was consistent across the position range of the detector, which is evidence that our detector was parallel to the focal plane. In our calibration, we find a slight quadratic shape between the position and bending radius. This is consistent with the fact that the focal plane is slightly curved. Furthermore, fitting these peaks with a Gaussian suggests a FWHM of 2.1 mm, which we take to be the position resolution of our detector. As previously stated, the energy resolution that corresponds to this position resolution will depend on the reaction, but is expected to be ~20-50 keV for most reactions of interest.

5.2 Particle Identification

To select ejectiles from the reaction channel of interest, particle identification (PID) is necessary. A plot of the energy deposited in the cathode vs. the focal plane position was found to be a particularly useful PID. A typical PID plot is shown in Figure 6a. The cathode energy has an associated non-linearity across the detector, which is thought to be caused by incomplete charge collection at certain points of the detector. The non-linearity of the alpha group is more pronounced, and this is likely due to the alpha particles liberating more electrons as they pass through the detector, making their cathode energy measurement more sensitive to the incomplete charge collection. However,

this non-linear shape is consistent throughout all runs, and we can therefore correct the cathode energy to create a more linear PID plot. An example of the PID plot with the cathode correction is shown in Figure 6b.

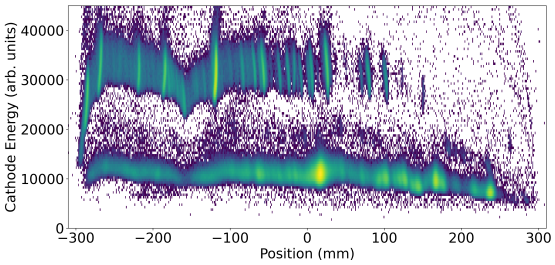

(a) Particle identification plot.

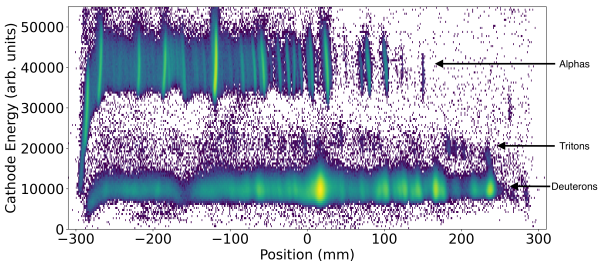

(b) Particle identification plot with cathode energy correction.

Figure 6: Example PID plots.

5.3 Focal Plane Calibration

The alpha particles originating from the (^{3}He,α) reaction on both ^{12}C and ^{58}Ni populate well known states in ^{11}C and ^{57}Ni, respectively. Peaks from these states provide points that can be used to simultaneously determine the magnetic field and entrance angle of the spectrograph. This is done in the following manner.

First, a grid of reasonable magnetic field strengths and opening angles are selected. From the calibration provided by the elastic scattering data, the positions of the particles are converted to bending radii. Then, for each magnetic field and angle pair, the bending radii of these states are converted to excitation energies. The squares of the residuals between the calculated level energies and known level energies are then determined. The magnetic field and angle pair that is chosen is the one with the minimum sum of these squares.

Once the magnetic field and entrance angle are determined for a given set of runs, a particle group can be selected by gating on cathode energy, and the ejectile energy can be determined. From the ejectile energy and reaction kinematics, the excitation energy of the compound nucleus can be determined. Preliminary results from the reaction of interest, ^{58}Ni(^{3}He,t)^{58}Cu, are shown in the following section.

5.4 Preliminary Results

By gating on tritons in the cathode vs. position plot, the tritons from the ^{58}Ni(^{3}He,t)^{58}Cu reaction can be selected. From the calibration method described above the triton energies, and therefore the excitation energies of ^{58}Cu, can be determined. An example spectrum of ^{58}Cu excitation energy taken at a laboratory entrance angle of 24.7° is shown in Figure 7. The black dotted lines represent states in ^{58}Cu that have been previously measured with low uncertainty (<10 keV), while the red dotted lines represent states in ^{58}Cu that were previously measured but with high uncertainty (>10 keV). There is good agreement between the experimental data and states with low uncertainty. Furthermore, the FWHM of the triton peaks is on the order of 30 keV, which will likely allow us to reduce the uncertainty in states with high uncertainty to ~ 3 keV.

Furthermore, peaks can be seen that do not correspond to known levels, most notably above 4 MeV. While the analysis is still ongoing, this could suggest additional levels in ^{58}Cu that may lead to significant resonances in the ^{57}Ni(p,γ)^{58}Cu reaction.

It should also be noted that the diode detectors were used in the present experiment. It is still too early in the analysis to determine whether they were able to detect a significant number of proton decays in ^{58}Cu, but, if they were, this could provide proton branching ratios for higher lying states. Triton spectra were also taken at multiple angles, and work is underway to extract angular distributions that could help constrain the spins of the states. The additional constraints on structure properties such as level energies, spins, and proton branching ratios should ultimately impact the experimental constraint of the rate.

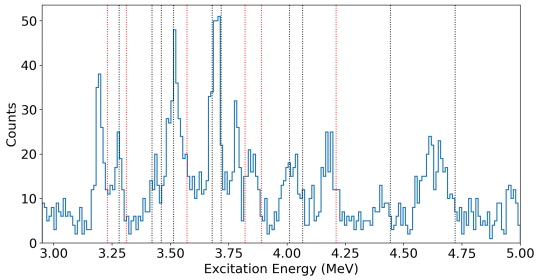

Figure 7: ^{58}Cu excitation energy spectrum taken at a laboratory angle of 24.7°. The black/red dotted lines represent states known in ^{58}Cu with low/high uncertainty.

6 Conclusion

To effectively constrain certain reaction rates that significantly impact nucleosynthesis in explosive astrophysical environments, it is necessary to measure the level energies of states in the compound nucleus that may lead to resonances. Further constraints can be placed on the reaction rate by determining the spins of these states, as well as their particle widths.

The Enge split-pole spectrograph is an ideal tool for this task, and one has been installed in the University of Notre Dame's Nuclear Science Laboratory. To measure the position of particles on the focal plane, an ionization chamber has been constructed. This ionization chamber is capable of measuring the position of ejectiles with a resolution of ~2.1 mm and provides particle identification that can distinguish between isotopes. This position resolution was determined by measuring elastic scattering of ^{3}He at 21 MeV, but should not be strongly dependent on particle energy. It may, however, depend on the particle species, as particles with a higher Z will liberate more electrons in the detector and produce stronger electric signals.

The first scientific measurement of the Enge split-pole spectrograph has taken place to probe the structure of ^{58}Cu using the ^{58}Ni(^{3}He,t)^{58}Cu reaction. Tritons ejected in the reaction were separated in the Enge split-pole spectrograph based on their magnetic rigidity. The energy of the tritons was determined by their position on the focal plane. From the energy of the tritons and reaction kinematics, the level energies of states in ^{58}Cu could be determined. Preliminary analysis is ongoing, but the measurement is expected to reduce the level energy uncertainty in states that will likely contribute to significant resonances, thereby constraining the astrophysical rate of ^{57}Ni(p,γ)^{58}Cu.

7 Acknowledgments

This research is supported by the University of Notre Dame, the National Science Foundation (grant no. PHY-2310059), and Brazilian National Council for Scientific and Technological Development (grant no. 200237/2023-3).

References

[1] C.E. Rolfs, W.S. Rodney, Cauldrons in the Cosmos (University of Chicago Press, Chicago, 1988)
[2] G. Magkotsios, F.X. Timmes, A.L. Hungerford, C.L. Fryer, P.A. Young, M. Wiescher, The Astrophysical Journal Supplement Series **191**, 66 (2010).
[3] K. Hermansen, S.M. Couch, L.F. Roberts, H. Schatz, M.L. Warren, The Astrophysical Journal **901**, 77 (2020).
[4] N. Nishimura, T. Rauscher, R. Hirschi, G. Cescutti, A.S.J. Murphy, C. Fröhlich, Monthly Notices of the Royal Astronomical Society **489**, 1379 (2019).
[5] S.K. Subedi, Z. Meisel, G. Merz, The Astrophysical Journal **898**, 5 (2020).
[6] C.D. Nesaraja, S.D. Geraedts, B. Singh, Nuclear Data Sheets **111**, 897 (2010).
[7] D.W. Bardayan, P.D. O'Malley, D. Robertson, E. Stech, M. Wiescher, AIP Conference Proceedings **2160**, 070008 (2019).
[8] J.E. Spencer, H.A. Enge, Nucl. Instrum. and Methods **49**, 181 (1967).
[9] E.C. Good, Ph.D. thesis (2020)
[10] T. Rounsaville, Tedector User's Manual (2004), unpublished